

## DISTANCES OF LOCAL CLOUDS FROM OPTICAL LINE OBSERVATIONS

Richard M. Crutcher and David J. Lien  
Astronomy Department, University of Illinois

### ABSTRACT

We observed the interstellar D-lines of Na I toward 49 stars in order to determine the distance ( $125 \pm 25$  pc) to a cold H I cloud. This sheet of gas may be part of the back side of the shell formed by the Loop I supernova.

### INTRODUCTION

Riegel and Crutcher (1972) and Crutcher and Riegel (1974) studied the angular extent and physical properties of an H I cloud detected as a narrow self-absorption feature in 21-cm line profiles. It is seen in self-absorption over  $345^\circ < l < 385^\circ$ ,  $|b| < 7^\circ$  and apparently also in emission at higher galactic latitude and lower longitude. Its typical properties are  $T_k = 30$  K,  $n(\text{H I}) = 100 \text{ cm}^{-3}$ ,  $N(\text{H I}) = 3 \times 10^{20} \text{ cm}^{-2}$ . Two separate velocity components are seen, at LSR velocities of +4 and +7  $\text{km s}^{-1}$ . Narrow molecular lines of OH and CO are sometimes observed at the same velocities, and the cold H I seems to be spatially correlated with the distribution of local dust clouds.

### OBSERVATIONS

In order to better define the distance of this cloud, observations of the optical interstellar Na I D-lines were made toward early-type stars in the direction of the cold cloud. The Na I lines are better tracers of denser gas than either the Ca II lines or color excess. The Varo-reticon detector on the coude spectrograph of the Mt. Wilson 2.5-m telescope was used. The velocity resolution was about  $10 \text{ km s}^{-1}$ , which was sufficient to exclude the possibility of stellar Na I lines with a high degree of confidence. The rms error in measured equivalent widths and the minimum detectable equivalent width were typically 10 mÅ and 20 mÅ, respectively. New observations of the 21-cm line of H I were also made at the position of each star with the 43-m telescope of the NRAO. The velocity resolution was  $0.4 \text{ km s}^{-1}$  and the beamsize was 20 arcmin. A strong optical interstellar line at the velocity of H I self-absorption was taken as evidence that the stellar distance was an upper limit to the distance of the cold cloud. Velocity differences of  $4\text{--}5 \text{ km s}^{-1}$  between Na I and H I are not significant because of the low spectral resolution of the optical data, the complexity of the background H I emission profiles, and the presence of multiple velocity components. Using a curve of growth with a velocity parameter  $b = 2.5 \text{ km s}^{-1}$ , we estimated column densities of Na I from the weaker D-line which was observed. Because of line saturation, these estimates are not particularly accurate; and any column density greater than  $10^{13} \text{ cm}^{-2}$  is given as a lower limit only. For the relative comparison purposes of this paper, this procedure is adequate.

Our results are given in the Table. Column headings are the HD number of the star, the galactic coordinates in degrees, the spectral type, the visual

magnitude and color, the color excess, the photometric distance derived from the preceding data, the equivalent widths in milliangstroms of the Na I  $D_1$  and  $D_2$  lines, the column density of Na I in units of  $10^{12} \text{ cm}^{-2}$ , the LSR radial velocity of the Na I and of the H I, and an index  $p$  which specifies the nature of the H I line. Figure 1 shows the H I profiles which are the prototypes of the H I classification index  $p$ . The very strong self-absorption feature toward HD163955 is  $p = 1$ , and the progressively weaker features as one moves clockwise in the Figure are of types 2 and 3. The lack of self-absorption seen toward HD154481 is  $p = 4$ ; in these cases the H I emission velocity is given. Some of the stars had missing luminosity type or photometric data. Although such stars are included in the Table, they are not used in the subsequent analysis.

## DISCUSSION

Figure 2 shows the Na I column densities plotted against stellar distance. The points begin to rise significantly at about 100 pc, and by 150 pc virtually all stars have strongly saturated interstellar Na I lines. Hence, our distance estimate for the cold cloud is  $125 \pm 25$  pc. Figure 3 shows the stellar distances plotted against galactic longitude. There is no clear evidence for part of the cloud being closer than other parts. However, at longitudes near  $20^\circ$  a distance near 100 pc seems most appropriate. For  $l < 360^\circ$  the distance is less well defined and may be up to 200 pc. There is therefore a fairly dense cloud of cold H I, dust, and molecules about 125 pc from the sun with an extent of at least 90 pc along the galactic plane. Since the thickness is 1-5 pc, the morphology is that of a sheet.

Berkhuijsen (1973) found a distance of  $130 \pm 75$  for the center of the Loop I supernova remnant; the corresponding radius of the remnant is 115 pc. The morphology of a cold sheet of gas lying within Loop I and oriented radially with respect to the center is rather unlikely. The observations of x-rays from this direction argue against the cold sheet being in front of Loop I. We suggest that the cold sheet forms part of the back side of the compressed shell of gas swept up by Loop I. If the distance of the sheet were 100 pc for  $l > 20^\circ$  and 150-200 pc for  $l < 0^\circ$ , which is perfectly compatible with our data, the morphology would fit this hypothesis very well.

Crutcher (1982) analyzed the velocities of published optical interstellar line data and showed that the sun is immersed in a coherently moving local interstellar medium which he identified with the solar system's interstellar wind. The velocity vector is consistent with this gas being the front side of the Loop I shell. The center of Loop I would then have a radial velocity with respect to the LSR of about  $-5 \text{ km s}^{-1}$  and an expansion velocity of about  $10 \text{ km s}^{-1}$ ; hence, the age would be  $< 10^7$  yr.

## REFERENCES

- Berkhuijsen, E.M. 1973, Astron.Ap., 24, 143.  
 Crutcher, R.M. and Riegel, K.W. 1974, Ap.J., 188, 481.  
 Crutcher, R.M. 1982, Ap.J., 254, 82.  
 Riegel, K.W. and Crutcher, R.M. 1972, Astron.Ap., 18, 55.

| HD     | l     | b    | Sp    | V    | B-V  | E <sub>B-V</sub> | dist | W <sub>D1</sub> | W <sub>D2</sub> | N(10 <sup>12</sup> ) | V <sub>Na</sub> | V <sub>H</sub> | P   |
|--------|-------|------|-------|------|------|------------------|------|-----------------|-----------------|----------------------|-----------------|----------------|-----|
| 148898 | 356.3 | 17.8 | A7p   | 4.46 | .12  | .00              | 30   | -               | -               | <0.2                 | -               | 2              | 3   |
| 149438 | 351.5 | 12.8 | B0V   | 2.83 | -.25 | .05              | 260  | 87              | 45              | 0.6                  | 6               | 5              | 3   |
| 150366 | 355.3 | 14.2 | F0V   | 6.06 | .22  | .00              | 50   | -               | -               | <0.2                 | -               | 4              | 1   |
| 150638 | 349.6 | 9.0  | B9    | 6.46 | -.08 | .00              | >240 | 62              | -               | 0.4                  | 3               | 4              | 2   |
| 150768 | 353.4 | 11.8 | A0    | 6.38 | -    | -                | >140 | -               | -               | <0.2                 | -               | 4              | 3   |
| 150894 | 352.6 | 11.1 | A2    | 5.96 | -    | -                | >90  | 74              | -               | 0.4                  | 4               | 4              | 4   |
| 151527 | 4.3   | 18.8 | A0V   | 6.03 | .20  | .20              | 90   | 254             | 214             | >10                  | -2              | 4              | 1   |
| 152909 | 1.6   | 14.4 | B6V   | 6.28 | .07  | .21              | 180  | 286             | 216             | >10                  | -4              | 5              | 2   |
| 153613 | 352.0 | 6.0  | B8V   | 5.03 | -.10 | .00              | 110  | -               | -               | <0.2                 | -               | 4              | 1   |
| 154204 | 1.9   | 12.4 | B6IV  | 6.30 | -.02 | .12              | 320  | 179             | 142             | 4.6                  | 9               | 4              | 3   |
| 154481 | 357.3 | 8.5  | A3IV  | 6.28 | .02  | .00              | 110  | 261             | 116             | 2.5                  | 11              | 5              | 4   |
| 155379 | 359.0 | 8.3  | A0    | 6.52 | -.01 | -                | >150 | 83              | 64              | 0.9                  | 0               | 5              | 4   |
| 155401 | 356.9 | 6.7  | B9    | 6.11 | .02  | -                | >180 | -               | -               | <0.2                 | -               | 4              | 1   |
| 156247 | 22.7  | 21.6 | B5V   | 5.70 | .07  | .23              | 160  | 219             | 164             | 9.5                  | 2               | 1              | 4   |
| 156325 | 353.8 | 2.9  | B6IV  | 6.37 | .14  | .28              | 270  | 241             | 192             | >10                  | 5               | 5              | 3   |
| 156717 | 6.3   | 11.0 | A2V   | 6.02 | .04  | .00              | 90   | -               | -               | <0.2                 | -               | 7              | 2   |
| 156928 | 10.6  | 13.5 | A1V   | 4.33 | .03  | .02              | 50   | -               | -               | <0.2                 | -               | 2              | 2   |
| 157056 | 0.5   | 6.6  | B2IV  | 3.28 | -.21 | .03              | 200  | 89              | 51              | 0.7                  | 0               | 4              | 1   |
| 157546 | 6.3   | 9.7  | A0V   | 6.37 | .00  | .00              | 140  | 201             | 147             | 5.4                  | 2               | 5              | 4   |
| 157792 | 1.7   | 6.2  | A9V   | 4.17 | .28  | .02              | 20   | -               | -               | <0.2                 | -               | 4              | 1   |
| 158643 | 2.5   | 5.4  | B9.5V | 4.81 | .00  | .03              | 70   | -               | -               | <0.2                 | -               | 4              | 1   |
| 158704 | 0.6   | 4.0  | B9p   | 6.08 | -.06 | -                | >200 | -               | -               | <0.2                 | -               | 4,7            | 1,2 |
| 159877 | 10.5  | 8.6  | A5V   | 5.94 | .37  | .22              | 180  | 514             | 509             | >10                  | 0               | 3              | 3   |
| 159975 | 17.0  | 12.3 | B8II  | 4.62 | .11  | .20              | 140  | 319             | 250             | >10                  | 7               | 4              | 1   |
| 161056 | 18.7  | 11.6 | B3V   | 6.28 | .38  | .58              | 180  | 483             | 440             | >10                  | 10              | 4              | 2   |
| 161701 | 12.4  | 6.9  | B9III | 5.95 | .01  | .07              | 170  | 167             | 93              | 1.6                  | 7               | 3              | 1   |
| 161840 | 358.0 | -2.1 | B8V   | 4.82 | -.04 | .05              | 100  | 156             | 88              | 1.5                  | 6               | 5,7            | 1,2 |
| 163318 | 2.0   | -1.6 | A3    | 5.72 | .21  | -                | >70  | -               | -               | <0.2                 | -               | 6              | 1   |
| 163336 | 12.5  | 4.6  | A1V   | 5.89 | .05  | .04              | 90   | -               | -               | <0.2                 | -               | 6              | 1   |
| 163955 | 6.0   | -0.1 | B9V   | 4.75 | -.05 | .01              | 80   | -               | -               | <0.2                 | -               | 7              | 1   |
| 164536 | 6.0   | -0.9 | O9III | 7.11 | -.03 | .28              | 2500 | 228             | 174             | >10                  | 6               | 7              | 1   |
| 165402 | 20.3  | 6.1  | B8IV  | 5.84 | .20  | .29              | 140  | 202             | 181             | >10                  | -1              | 4              | 1   |
| 165814 | 5.6   | -2.7 | B4V   | 6.66 | .04  | .22              | 300  | 229             | 173             | >10                  | 4               | 7              | 1   |
| 166393 | 10.8  | 0.5  | A4V   | 6.36 | .16  | .04              | 80   | 126             | 51              | 0.7                  | 10              | 7              | 1   |
| 166937 | 10.0  | -1.6 | B8Ia  | 3.85 | .22  | .24              | 1100 | 253             | 180             | >10                  | 9               | 6              | 1   |
| 167666 | 3.7   | -5.9 | A4    | 6.12 | .16  | -                | >70  | 233             | 162             | 9.0                  | 7               | 6              | 4   |
| 167833 | 20.3  | 3.0  | A5III | 6.30 | .38  | .23              | 130  | 150             | 132             | 3.6                  | 8               | 4              | 3   |
| 169033 | 19.0  | 0.7  | B8V   | 5.73 | .01  | .10              | 150  | 190             | 168             | >10                  | 6               | 5              | 1   |
| 169990 | 14.5  | -3.0 | B8V   | 6.03 | .01  | .10              | 150  | 189             | 148             | 5.6                  | -2              | 7              | 2   |
| 170296 | 17.5  | -1.8 | A3V   | 4.70 | .06  | .00              | 40   | 116             | 93              | 1.6                  | 1               | 3              | 4   |
| 170680 | 14.3  | -4.0 | A0V   | 5.14 | .00  | .00              | 80   | -               | -               | <0.2                 | -               | 7              | 3   |
| 170740 | 21.1  | -0.5 | B2V   | 5.91 | .27  | .51              | 240  | 234             | 189             | >10                  | 5               | 4,8            | 1,1 |
| 170902 | 17.7  | -2.5 | A4V   | 6.37 | .22  | .10              | 80   | 87              | 74              | 1.1                  | 4               | 4              | 3   |
| 171130 | 17.7  | -2.9 | A2V   | 5.76 | .04  | .00              | 80   | -               | -               | <0.2                 | -               | 4              | 4   |
| 171957 | 18.9  | -3.5 | B9IV  | 6.40 | .21  | .27              | 140  | 346             | 346             | >10                  | 9               | 4              | 3   |
| 171961 | 10.5  | -7.8 | B9    | 5.75 | .02  | -                | >170 | 179             | 129             | 3.4                  | 5               | 5              | 4   |
| 175156 | 19.3  | -7.7 | B5III | 5.08 | .17  | .33              | 150  | 351             | 279             | >10                  | 6               | 6              | 2   |
| 175623 | 20.2  | -7.9 | B9    | 7.15 | .22  | -                | >320 | 351             | 304             | >10                  | 3               | 6              | 3   |
| 176162 | 22.3  | -7.6 | B5IV  | 5.53 | -.04 | .12              | 170  | 201             | 171             | >10                  | -1              | 3              | 4   |

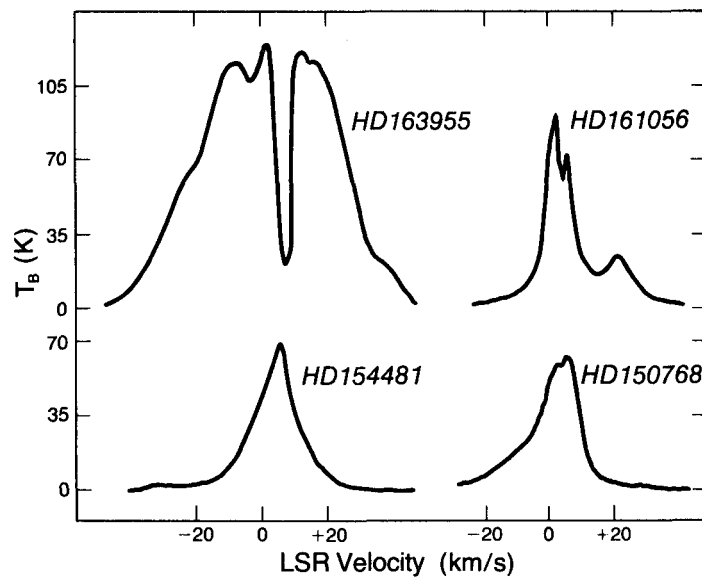


Figure 1 - Examples of the H I line profiles.

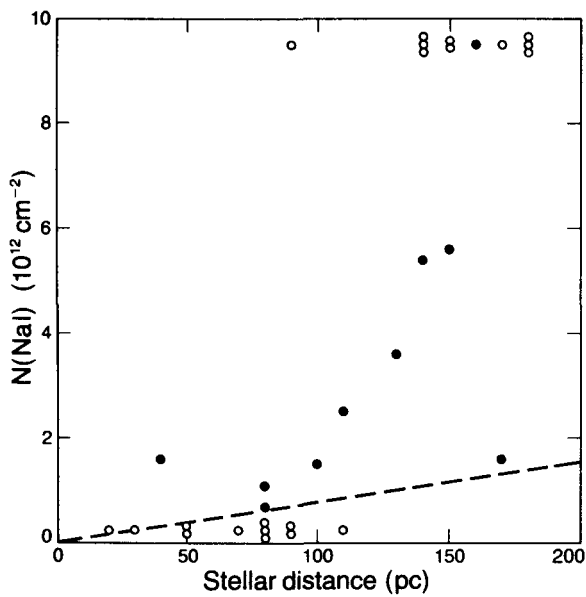


Figure 2 - Na I column density versus stellar distance. The open circles represent lower and upper limits on  $N(\text{Na I})$ .

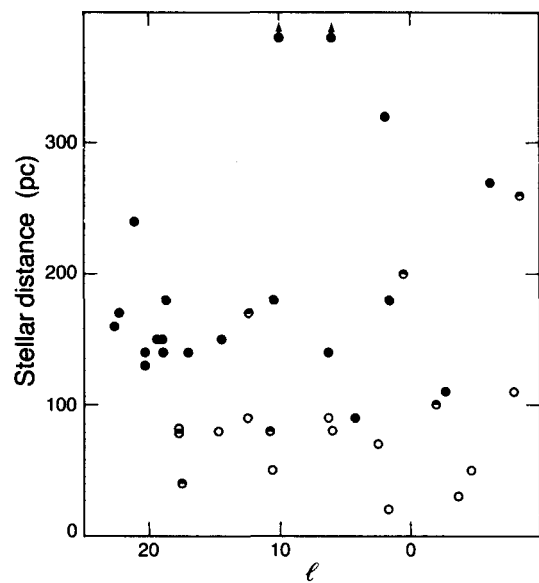


Figure 3 - The open and filled circles represent  $N(\text{Na I}) < 0.2$  and  $> 2 \times 10^{12} \text{ cm}^{-2}$ , respectively. The intermediate cases are half-filled.